# Mathematical Model of Turbojet Engine Combustion Chamber Primary Zone

**Nikola Davidović**
Research Assistant
University of Belgrade
Faculty of Mechanical Engineering

*Mathematical model of turbojet engine primary zone was developed and tested. Combustion chamber was of annular type with single annular vaporizer positioned at the center. This configuration is very attractive for the applications where small dimensions are of primary interest. The model was tested as a part of combustion chamber and it was estimated through the overall combustion chamber efficiency.*

***Keywords :*** *combustion chamber, vaporizer, primary zone, turbojet.*

## 1. INTRODUCTION

Mathematical model of turbojet engine combustion chamber primary zone was developed and verified by test. Combustion chamber was of annular type with a single annular vaporizer positioned at the center. This configuration is very attractive for applications where small dimensions are of primary importance. The model was tested as a part of whole combustion chamber, i.e. not in the laboratory, but in real conditions. Results show good agreement with proposed logic of mathematical model.

## 2. MODEL DESCRIPTION

The model scheme is shown in the figure 1. The model consists of annular vaporizer positioned at the center of primary zone and primary zone which length can be greater or equal to the length of the vaporizer. Such configuration meets both demands for small overall dimensions and for low emission, as it can be seen from references [1] and [2]. Geometrical values which are included into the mathematical model are diameter and length of the primary zone and vaporizer.

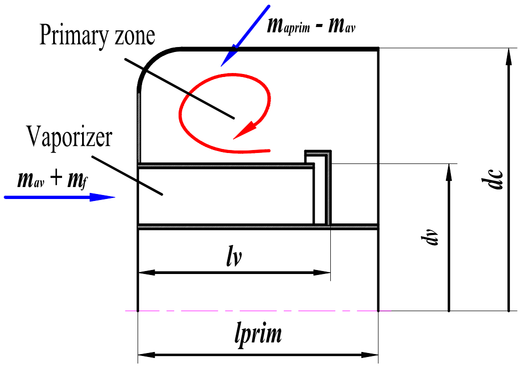

**Figure 1. Scheme of the model**

The idea is to use the ratio of residence time and time needed for characteristic process for estimation of the process quality or, inversely, for the desired quality to determine geometry. That idea, called characteristic time model, is not new but new is this model treatment.

Quality of the process, besides geometry, is affected by various parameters. They can be divided upon the source, as it is shown in the figure 2.

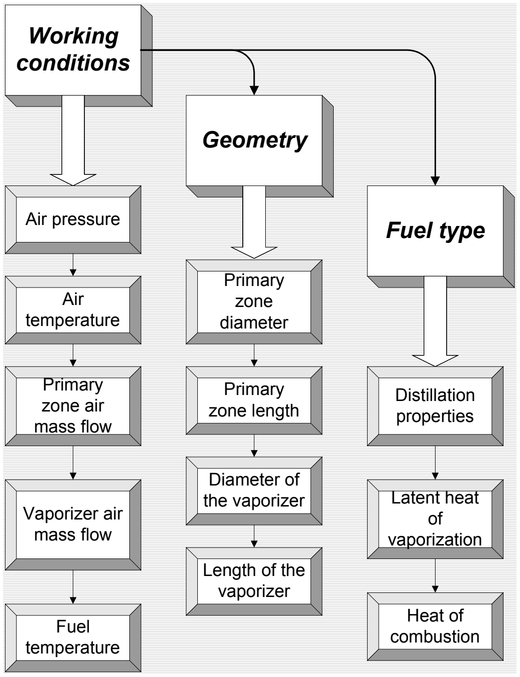

**Figure 2. Categorization of input values**

The logic of the model treating is schematically shown in the figure 3. Air and fuel in the liquid state, under certain working conditions, are entering the vaporizer. Under heating flux from primary zone and under mixing of the air and fuel, fuel is heated and partially vaporized. Quality of the process in the vaporizer is then estimated upon the ratio of residence time and time needed for the fuel to vaporize completely. The ratio of these times is actually probability for the process to be completely finished. The mixture of the air, liquid and vaporized fuel is then entering primary zone. In the primary zone liquid fuel is vaporizing, mixing with air and previously vaporized fuel, and finally burning. Estimation of these processes

Received: March 2007, Accepted: May 2007
*Correspondence to:* Nikola Davidović
Faculty of Mechanical Engineering,
Kraljice Marije 16, 11120 Belgrade 35, Serbia
E-mail: edepro@Eunet.yu

is done via the ratio of residence time and time needed for droplet vaporization and time for chemical reaction. Because all primary zone processes are going on simultaneously, it is possible that limiting is one process or combination of the processes or all. Probabilities of all characteristic processes are giving complete estimation of the system quality. This estimation should be experimentally corrected for the particular model.

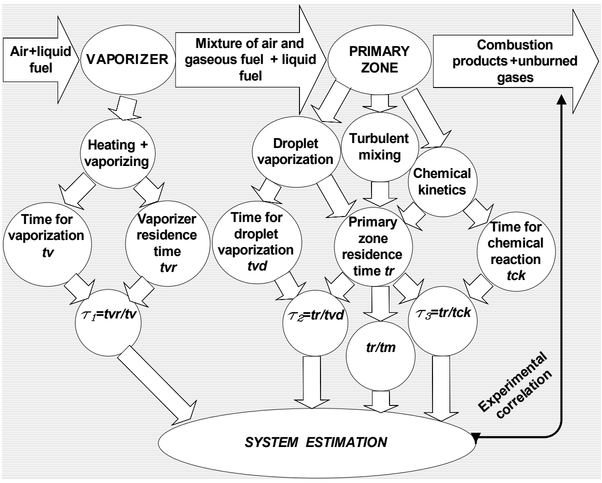

**Figure 3. Scheme of the model treating**

In this model turbulent mixing of the fuel and air was not considered because velocity and pressure drop were on the upper limits of the existing combustion chambers, so the assumption is that mixing process is very intensive and not the one limiting the analyzed process.

## 3. CORRELATION OF THE PARAMETERS $\tau_1$, $\tau_2$ AND $\tau_3$ WITH COMBUSTION CHAMBER PERFORMANCES

Values of the parameters $\tau_1$, $\tau_2$ and $\tau_3$ show the influence intensity on the particular process. If they are greater than unity, it means that there is enough time and there is great probability for the process to be finished and that process is not the one limiting the system. If they are less than unity, it means that is not enough time for the characteristic process to be finished completely and it is limiting to the system. So,

$$\tau_1 = \begin{cases} \tau_1, \text{ for } \tau_1 < 1 \\ 0.995 \ \text{, for } \tau_1 > 1 \end{cases}$$
$$\tau_2 = \begin{cases} \tau_2, \text{ for } \tau_2 < 1 \\ 0.995 \ \text{, for } \tau_2 > 1 \end{cases} \qquad (1)$$
$$\tau_3 = \begin{cases} \tau_3, \text{ for } \tau_3 < 1 \\ 0.995 \ \text{, for } \tau_3 > 1 \end{cases}.$$

Instead of parameter $\tau_1$ in the model was used mass ratio of the fuel vaporized in the vaporizer to the total mass of the fuel because it shows more real picture of the process. Actually, when the air inlet temperature is lower than end vaporization temperature of the fuel, then parameter $\tau_1$ incorporates heating of the air, while air is actually cooled due to fuel heating, so the actual percentage of vaporized fuel is bigger. Upon previous considerations efficiency of the combustion chamber can be shown as

$$\eta_g \approx \left[p + (1-p)\cdot\tau_2\right]\cdot\tau_3 . \qquad (2)$$

Logic of the equation (2) is simple: the fuel vaporized in vaporizer does not affect parameter $\tau_2$, which estimates the vaporization in primary zone, and vice versa. Because of the assumptions which are related to the exact determination of parameters, some corrective factor can be applied, i.e.

$$\eta_g = \left[a\cdot p + (1-a\cdot p)\cdot b\cdot\tau_2\right]\cdot c\cdot\tau_3 \qquad (3)$$

or

$$\eta_g = \left[a\cdot p\cdot(1-b\cdot\tau_2) + b\cdot\tau_2\right]\cdot c\cdot\tau_3 . \qquad (4)$$

Corrective coefficients *a, b* and *c* are determined by experiment.

Equation (2) is very interesting: when $p>0$ efficiency is higher because of previously vaporized fuel ($p$) and because of preheated fuel which affects parameter $\tau_2$. If we differentiate equation (2) with parameter $p$

$$\frac{d\eta_g}{dp} = (1-\tau_2)\cdot\tau_3 . \qquad (5)$$

From equation (5) we may conclude that when parameter $\tau_2$ is equal to the unity, i.e. if the droplets are small enough or residence time big enough, pre-vaporized fuel is not strongly affecting the efficiency, and opposite, if the parameter $\tau_2$ is close to the zero, effect of the pre-vaporized fuel is maximal. Conclusion is quite logic, there is not need for vaporizer when the fuel atomization is very good, and vice versa. However, it is possible to minimize combustion chamber dimensions by combining the effects of vaporizing and atomization. It is a dominant request for the flying jet engines, especially to the engines with low pressure ratio.

### 3.1 Description and definition of the parameters $\tau_1$, $\tau_2$ and $\tau_3$

Parameters $\tau_1$, $\tau_2$ and $\tau_3$ have physical meanings:

Parameter $\tau_1$ is the ratio of the air and fuel residence time in vaporizer to the time needed for fuel to vaporize. Numerical value in the model for the parameter $\tau_1$ represents mass ratio of the fuel vaporized in vaporizer $p$. It is derived from vaporizer energy equation [2]. Convective and emissive heat flux from primary zone is used for heating the fuel to the beginning of vaporization, then for vaporizing fuel, heating fuel in liquid and gaseous state to the exit temperature and, finally to heat the air to the exit temperature, as it is written in equation (6).

$$(q_e + q_{con})A_v = m_f \Big[ \int_{T_f}^{T_{sv}} C_f(T)dT +$$

$$\int_{T_{sv}}^{T_{ev}} \frac{\mathrm{d}p(T)}{\mathrm{d}T} L_t(T)\mathrm{d}T + \int_{T_{sv}}^{T_{ev}} [1-p(T)]C_f(T)\mathrm{d}T + \qquad (6)$$

$$\int_{T_{sv}}^{T_{ev}} \cdot p(T) C_{Pfg}(T)\mathrm{d}T \Big] + m_{av} \int_{T_a}^{T_{ev}} C_{Pair}(T)\mathrm{d}T.$$

Emissive and convective heat flux from primary zone are determined as

$$q_e = \frac{1+\varepsilon_w}{2} \sigma\varepsilon_g T(\varphi_{prim},\eta_g)^{1.5}\left[T(\varphi_{prim},\eta_g)^{2.5} - T_w^{\;2.5}\right] \qquad ,(7)$$

$$q_{con} = 0.017 \frac{\lambda_g}{D_h^{0.2}} \left(\frac{m_{aprim}}{A_{prim}\mu_g}\right)^{0.8}\left[T(\varphi_{prim},\eta_g) - T_w\right], \qquad (8)$$

$$\tau_1 \equiv p\,. \qquad (9)$$

Parameter $\tau_2$ is the ratio of mixture residence time in primary zone to the time needed for droplet vaporization. Droplet diameter is determined as for airblast-type injector, as it was mentioned in the reference [3].

$$\tau_2 = \frac{t_f}{t_{ik}} = \frac{\dfrac{L^*}{\Gamma(\kappa_g)\sqrt{R_g\,T(\varphi_{prim},\eta_g)}}}{\dfrac{D_o^2}{k}}\,. \qquad (10)$$

Parameter $\tau_3$ is the ratio of mixture residence time in primary zone to the time needed for chemical reaction. Direct equation of parameter $\tau_3$ can be found in references [3] and [4], but numerical value in the model for the parameter $\tau_3$ represents combustion chamber efficiency. The reason for that change is both numerical and physical: better numerical agreement with test while the origin of that efficiency is the assumption that chemical reaction is the one limiting the process in combustion chamber, so

$$\log\left[\log\left(\frac{100}{\eta_g}\right)\right] = A\log\left[\frac{m_f}{P_c^n V} tk(\varphi,T_a)\right] + B\varphi^m + C(\kappa), \qquad (11)$$

$$\tau_3 \equiv \eta_g\,. \qquad (12)$$

Efficiency is then iteratively calculated by combining equations (6), (7), (8), (10) and (11) into equation (4). More detailed explanations of parameters can be found in reference [3].

## 4. TEST

### 4.1 Measuring points

Measuring points are shown in the figure 4. Air and fuel mass flow rate and fuel temperature are input values measured at the installation. Efficiency is not measured directly, but in a manner of rocket combustion chambers. That is,

$$m_a + m_f = \frac{P_{ex}^*}{C^*} \cdot \frac{A_c}{A_{ex}} \cdot A_{ex} \qquad (13)$$

variables in previous equation are defined as

$$C^* = \frac{\sqrt{R_g \cdot T_{ex}(\varphi,\eta_g)}}{\Gamma(\kappa_g)}\,,$$

$$\Gamma(\kappa_g) = \sqrt{\kappa_g} \cdot \left(\frac{2}{\kappa_g + 1}\right)^{\frac{\kappa_g+1}{2\cdot(\kappa_g-1)}}\,,$$

$$\frac{A_c}{A_{ex}} = \frac{\left(\dfrac{p_e}{P_{ex}^*}\right)^{\frac{1}{\kappa_g}} \cdot \sqrt{\dfrac{\kappa_g+1}{\kappa_g-1}\left[1-\left(\dfrac{p_e}{P_{ex}^*}\right)^{\frac{\kappa_g-1}{\kappa_g}}\right]}}{\left(\dfrac{2}{\kappa_g+1}\right)^{\frac{\kappa_g-1}{\kappa_g}}}\,,$$

with critical conditions at the exit equation (13) becomes

$$m_a + m_f = \sqrt{\frac{\kappa_g}{R_g}}\left(\frac{2}{\kappa_g+1}\right)^{\frac{\kappa_g+1}{2(\kappa_g-1)}} \frac{P_{ex}^*}{\sqrt{T_{ex}(\varphi,\eta_g)}} A_{ex}\,. \qquad (14)$$

Gas properties in above equations corresponds to the exit conditions. On the other side, it can be assumed that gas properties are constant for the typical range of exit temperatures. Then efficiency can be calculated by measuring $m_a$, $m_f$ and $P_{ex}^*$. So,

$$\eta_g = \frac{m_{fef}}{m_f} \approx \frac{T_{ex} - T_a}{T_{id} - T_a}\,. \qquad (15)$$

Efficiency measured in that manner is especially suited for primary and secondary zone tests, when exit temperatures are very high. It should be noted that for more precise measurement it is necessary to control the temperature of the exit cross section material due to thermal dilatation.

### 4.2 Measuring equipment

Pressures were measured with pressure transducers type PX602 and differential pressure transducers type PX126 and PX142, produced by Omega®. Temperatures at the air and fuel installation were measured with thermocouples type PT100, while temperatures at the testing object were measured with K-type thermocouples, all produced by Omega®. Fuel flow rate was measured with turbine flow meter produced by Ametek®. Acquisition of measured values were performed with equipment made in the Laboratory for Jet Propulsion from Faculty of Mechanical Engineering, University of Belgrade.

### 4.3 Geometry of tested models

Geometry of tested models of vaporizer and primary zone is shown in the figures 5 and 6. Models were tested in assembly with whole combustion chamber, as it is shown in the figure 4. That means working conditions were not simulated, but real. The photo of the combustion chamber with model I and model II alone is shown at the figure 7.

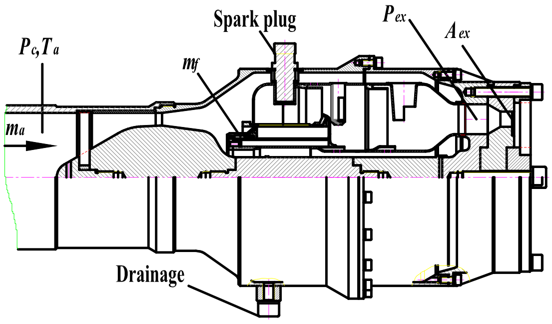

**Figure 4. Model II in assembly with whole combustion chamber at the testing installation**

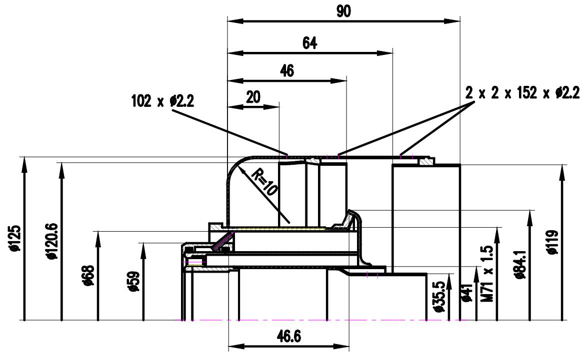

**Figure 5. Model I**

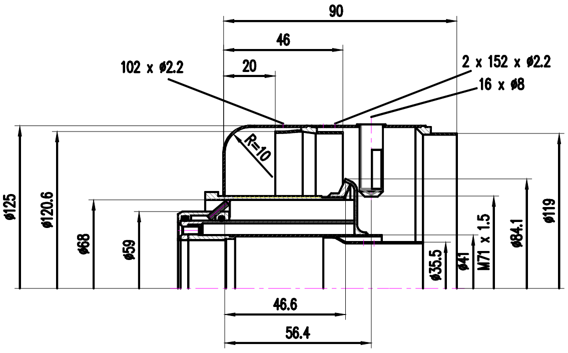

**Figure 6. Model II**

**Figure 7. Photo of whole combustion chamber with Model I and without dilution zone with Model II**

## 5. MATHEMATICAL MODEL AND TEST RESULTS

Models were tested at the two characteristic regimes, which corresponds to the starting and working regime of this combustion chamber.

Regime 1: $m_a = 400$ g/s , $T_a = 330$ K , $P_c = 1.4$ bar .

Regime 2: $m_a = 800$ g/s , $T_a = 423$ K , $P_c = 2.8$ bar .

Distribution of the air to the vaporizer and primary zone was determined at tests without combustion and it was used for determination of primary zone equivalence ratio in hot test. For both models 10.5% of the total air flow is passing through the vaporizer, while 21% of the air is passing through the primary zone.
The results from mathematical model are shown together with the test.

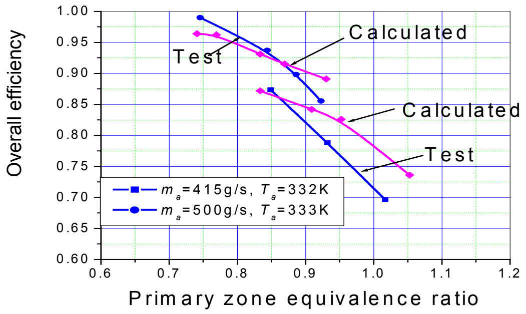

**Figure 8. Model I efficiency vs. primary zone equivalence ratio, regime 1**

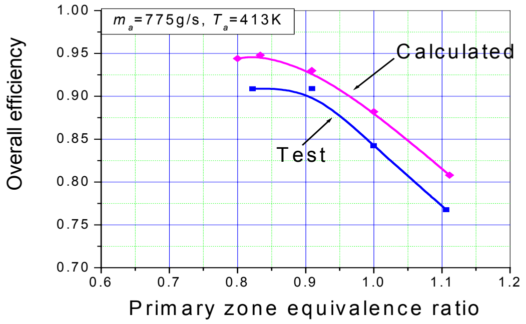

**Figure 9. Model I efficiency vs. primary zone equivalence ratio, regime 2**

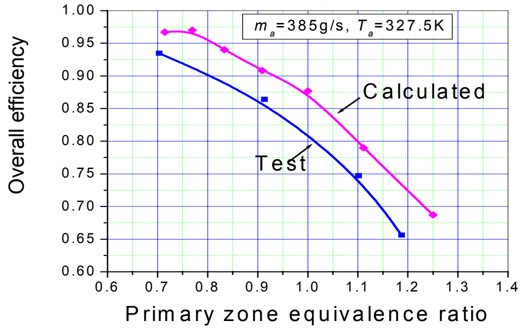

**Figure 10. Model II efficiency vs. primary zone equivalence ratio, regime 1**

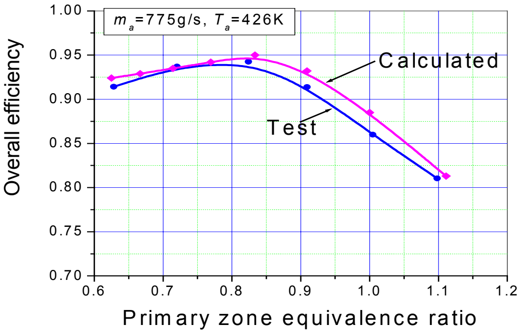

**Figure 11. Model II efficiency vs. primary zone equivalence ratio, regime 2**

### 5.1 Result comments

Figure 8 shows the results of calculation and test of the Model I at the regime 1 and at regime where air mass flow was increased to 500g/s. Curve has unique character for both air mass flows, but higher efficiencies correspond to the higher values of mass flow, approximately 0.06. This indicates the stronger effect of smaller drop diameter than smaller residence time. Curve shows the trend to reach maximum at the poor mixtures, at approximately 0.67. Calculated values are higher by about 0.06 in the area where equivalence ratio is greater than 0.9, while variation in poor zone is neglected.

Figure 9 shows the results of the Model I at regime 2. Maximum efficiency is reached at the primary zone equivalence ratio of 0.83. Calculated results follow this trend, with values higher by 0.03.

Figure 10 shows tested and calculated results of the Model II at the regime 1. Test and calculated results have the same trend, with numerical values difference less than 10%. It should be noted that this difference could be minimized if each model has its own numerical coefficients. As it is shown in the tables 1 and 2, both models have the same coefficients in order to make mathematical model more generalized.

Results of Model II at the regime 2 are presented in the figure 11. In contrast the regime 1, maximum efficiency is reached at the equivalence ratio of 0.83. As for the Model I, the difference between test and calculation is smaller at the regime 2, due to poor working conditions of the vaporizer at the regime 1.

Calculated curves were derived from equation (4) with coefficients a, b and c equal to one. Other coefficients are shown in the tables 1 and 2.

**Table 1. Regime 1**

| / | A | B | C | m | n |
|---|---|---|---|---|---|
| $0.5 \le \varphi_{prim} < 1$ | 0.911 | -1.1 | -1.64 | -1 | $2\varphi_{prim}$ |
| $1 \le \varphi_{prim} < 2$ | 0.911 | -1.1 | -0.89 | 1 | $2/\varphi_{prim}$ |

**Table 2. Regime 2**

| / | A | B | C | m | n |
|---|---|---|---|---|---|
| $0.5 \le \varphi_{prim} < 0.83$ | 0.911 | -1.1 | -1.64 | -1 | $2\varphi_{prim}$ |
| $0.83 \le \varphi_{prim} < 2$ | 0.911 | -1.1 | -0.40 | 1 | $2/\varphi_{prim}$ |

## 6. CONCLUSION

Primary zone function has most important influence on stability and efficiency of combustion chamber. Because of that, mathematical model was focused on primary zone. On the other side, efficiency of the whole combustion chamber is of practical importance, so the model was estimated through the overall combustion chamber efficiency. The main conclusions and contributions which can be taken from this investigation are:

- Correlation between mathematical model and test was established and it can be used with engineering acceptance for design of similar models.
- Vaporizer was not treated separately, but as a part of combustion chamber. It results in real testing conditions and the scope was not to have efficient vaporizer, but to have efficient combustion chamber.
- Somehow forgotten manner to estimate the efficiency via characteristic velocity was successfully used.
- Mathematical model which connects vaporizer and combustion chamber in unique system was established. Tests proved correct logic of the mathematical model.

## REFERENCES

[1] Ohkubo, Y.: Low-NOx combustion technology, R&D review of Toyota CRDL Vol.41 No.1, pp.12-23, Japan, 2005.

[2] Kumakura, H., Maekawa, H., Murakami, K.: Development of portable gas turbine generator ”Dynajet 2.6”, IHI Engineering Review Vol.37 No.3, pp. 113-115, Japan, 2004.

[3] Davidović, S.N., *Research of the central vaporizer characteristics of turbojet annular combustion chamber*, Ph. D. Thesis, Faculty of Mechanical Engineering University of Belgrade, 2003. (in Serbian)

[4] Roke, P.E., Hustad, J.E., Roke, N.A, Svensgaard, O.B.: Technology update on gas turbine dual fuel, dry low emission system combustion systems, Proceedings of ASME TURBO EXPO, ASME GT-2003-38112, Atlanta, 2003.

## NOMENCLATURE

| | |
|---|---|
| $A_c$ | Critical cross section [m$^2$] |
| $A_{ex}$ | Exit cross section [m$^2$] |
| $A_v$ | Heated surface of the vaporizer [m$^2$] |
| $A_{prim}$ | Axial cross section of primary zone [m$^2$] |
| $C^*$ | Characteristic velocity [m/s] |
| $C_f$ | Specific heat of the fuel in liquid state [J/kg] |
| $C_{Pfg}$ | Specific heat of the fuel in gaseous state at constant pressure [J/kg] |
| $C_{Pair}$ | Specific heat of the air at constant pressure [J/kg] |

| | |
|---|---|
| $d_c$ | Combustion chamber diameter [m] |
| $d_v$ | Vaporizer diameter [m] |
| $D_h$ | Hydraulic diameter of primary zone [m] |
| $D_o$ | Fuel droplet diameter [μm] |
| $k$ | Constant of droplet vaporization [m$^2$/s] |
| $l_{prim}$ | Length of primary zone [m] |
| $l_v$ | Length of the vaporizer [m] |
| $L^*$ | Primary zone characteristic length [m] |
| $L_t$ | Fuel latent heat of vaporization [J/kg] |
| $m_f$ | Fuel mass flow rate [kg/s] |
| $m_{fef}$ | Fictive fuel mass flow rate [kg/s] |
| $m_a$ | Total air mass flow rate [kg/s] |
| $m_{av}$ | Mass flow rate of the air through the vaporizer [kg/s] |
| $m_{aprim}$ | Mass flow rate of the air through the primary zone [kg/s] |
| $p$ | Mass fraction of the fuel vaporized in vaporizer |
| $P_c$ | Combustion chamber pressure [Pa] |
| $P_{ex}{}^*$ | Total pressure at the combustion chamber exit [Pa] |
| $p_e$ | Static pressure at the combustion chamber exit [Pa] |
| $R_g$ | Gas constant of combustion gases [J/kgK] |
| $t_{ck}$ | Time of chemical kinetics [s] |
| $t_r$ | Primary zone residence time [s] |
| $t_v$ | Time for fuel vaporization in vaporizer [s] |
| $t_{vr}$ | Vaporizer residence time [s] |
| $t_{vd}$ | Time needed for droplet to vaporize in primary zone [s] |
| $tk(\varphi, T_V)$ | Corrective function for combustion efficiency |
| $T_a$ | Temperature of the air [K] |
| $T_{ev}$ | Temperature of the air and fuel mixture at the vaporizer exit [K] |
| $T_f$ | Temperature of the fuel [K] |
| $T_{id}$ | Ideal combustion temperature [K] |
| $T_{sv}$ | Temperature of the start of fuel vaporization [K] |
| $T_w$ | Temperature of the vaporizers wall [K] |
| $T(\varphi_{prim}, \eta_g)$ | Primary zone temperature [K] |
| $q_{con}$ | Convective heat flux from primary zone to vaporizer [W/m$^2$] |
| $q_e$ | Emissive heat flux from primary zone to vaporizer [W/m$^2$] |
| $V$ | Combustion chamber volume [m$^3$] |

***Greek symbols***

| | |
|---|---|
| $\varepsilon_g$ | Emissive constant of the combustion gases |
| $\varepsilon_w$ | Emissive constant of the vaporizer wall |
| $\varphi$ | Overall equivalence ratio |
| $\varphi_{prim}$ | Primary zone equivalence ratio |
| $\Gamma(\kappa_g)$ | Gas-dynamic function |
| $\kappa_g$ | Ratio of specific heat at constant pressure to the constant volume of combustion gases |
| $\eta_g$ | Combustion efficiency |
| $\lambda_g$ | Conductivity of the combustion gases [W/mK] |
| $\mu_g$ | Dynamic viscosity of the combustion gases [Ns/m$^2$] |
| $\tau_1$ | Characteristic parameter of the process in vaporizer |
| $\tau_2$ | Characteristic parameter of the process of droplet vaporization in primary zone |
| $\tau_3$ | Characteristic parameter of the chemical reaction in primary zone |
| $\sigma$ | Stefan-Boltzmann constant [W/m$^2$K$^4$] |

---

## МАТЕМАТИЧКИ МОДЕЛ ПРИМАРНЕ ЗОНЕ КОМОРЕ САГОРЕВАЊА ТУРБОМЛАЗНОГ МОТОРА

**Никола Давидовић**

Развијен је и експериментално потврђен математички модел примарне зоне коморе сагоревања турбомлазног мотора. Комора сагоревања је прстенаста са прстенастим јединичним испаривачем постављеним централно у примарну зону. Оваква конфигурација је врло интересантна за апликације код којих су доминантни захтеви за малим димензијама. Модел је испитиван у склопу целе коморе сагоревања и оцењиван је преко потпуности сагоревања целе коморе.